DOI 10.5012/bkcs.2011.32.2.389

Accounts

Reactive Ion Scattering of Low Energy Cs^+ from Surfaces. A Technique for Surface Molecular Analysis

Heon Kang

Department of Chemistry, Seoul National University, Seoul 151-747, Korea. E-mail: surfion@snu.ac.kr
Received December 11, 2010, Accepted December 28, 2010

Although the currently available surface spectroscopic techniques provide powerful means of studying atoms and simple molecules on surfaces, the identification of complex molecules and functional groups is a major concern in surface analysis. This article describes a recently developed method of surface molecular analysis based on reactive ion scattering (RIS) of low energy (< 100 eV) Cs^+ beams. The RIS method can detect surface molecules *via* a mechanism in which a Cs^+ projectile picks up an adsorbate from the surface during the scattering process. The basic principles of the method are reviewed and its applications are discussed by showing several examples from studies of molecules and their reactions on surfaces.

Key Words: Surface analysis, Ion scattering, Mass spectrometry, Catalytic reaction, Ice

Introduction

Since the emergence of various surface spectroscopic methods based on the interactions of electrons, photons, and ions with surfaces in vacuum in the late 20th century,[1] the trend in surface science research has shifted gradually from the study of bare surfaces, to adsorbed atoms, and to molecules. Now, it is possible to characterize atoms and simple molecules adsorbed on surfaces almost on a routine basis, owing to the many powerful surface spectroscopic techniques developed to date. Yet, it is difficult to identify and characterize complex molecules and functional groups on surfaces, and this remains a major challenge for surface analysis. The need for surface molecular analysis is expected to increase in the future in relation to the research prospects of heterogeneous catalysis, molecular nanotechnology, and bio-mimetic materials.

Recently, a surface analysis technique based on the reactive scattering of Cs^+ ions at low energies (< 100 eV), called reactive ion scattering (RIS), has been developed.[2-18] In general, RIS refers to a variety of ion scattering experiments that exploit reactive processes taking place between active projectile ions and surfaces. The reactive processes include ion-surface charge exchange, the dissociation of molecular projectiles, transfer of an atom or functional moiety between a projectile ion and a surface, *etc*. Some of these topics have already been reviewed.[19,20,21,22] Here, we focus on the RIS process of low energy Cs^+ projectiles, which has particular significance for surface analysis among various RIS experiments. The RIS phenomenon was discovered first on a Si surface onto which water molecules had been adsorbed, where Cs^+ projectile ions scattering from the surface picked up water molecules to form Cs^+-water complexes.[2] Since then, the RIS process has been examined on various surfaces and molecular adsorbate systems,[2-18,23-47] and the RIS mechanism has been investigated theoretically by using molecular dynamics simulations.[48-53] These studies indicate that the nature of the RIS process is quite universal and, therefore, it can be applied to the analysis of molecules on surfaces.

The purpose of this review is to provide researchers in the surface science community with the basic information necessary to use RIS for surface analysis. For this reason, the RIS method is described with particular emphasis on basic principles and practical knowledge. Numerous RIS study results in the literature are either skipped over or discussed only minimally. It may be desirable for readers to have a background knowledge of ion-surface scattering kinematics, but this information can be found in other places.[54,55] Early RIS studies have been reviewed in a chapter of a monograph,[55] to which this author has provided an outline. Since then, RIS study has made a lot of progress, including a rigorous theoretical understanding of the RIS mechanism and its expanding applications in surface science research. These topics are the main subject of the present review, and they will be presented in the following sequence. Section (2) addresses the basic principles of RIS in its three aspects, i.e. (2.1) the nature of heavy ion-surface scattering at low energies, (2.2) the mechanisms of RIS and the associated low-energy sputtering (LES) process, and (2.3) experimental information which includes the apparatus, the modes of operation, and the quantification of RIS measurements. Section (3) presents a few case examples of surface science studies to which RIS has been

Heon Kang leads a surface science research group at Seoul National University (SNU). He received his BSc from SNU and a Ph.D. in Physical Chemistry from the California Institute of Technology for his study of gas-phase ion chemistry under the supervision of Prof. Jack Beauchamp. After working on low-energy ion-surface interactions as a postdoc with Prof. J. Wayne Rabalais at the University of Houston, he joined the chemistry faculty of Pohang University of Science and Technology in 1987. In 2001 he moved to SNU, where he is currently the director of the Center for Space-Time Molecular Dynamics. He is a recipient of Taikyue Ree Academic Award (2008) of the Korean Chemical Society.

applied, including the kinetic studies of catalytic reactions on a Pt surface (Sect. 3.1) and the studies of molecules on cold ice surfaces and their reactions (Sect. 3.2). Section (4) summarizes the main features of the RIS technique.

Principles of Reactive Ion-Surface Scattering

The Nature of Heavy Ion-Surface Scattering at Low Energies (< 100 eV). The ion-surface scattering phenomena at low collision energies (< 100 eV) are quite different from those at high energies (> 1 keV). When ion incident energy is greater than ~1 keV, the ion-surface collision process can be approximated as binary collisions (BCs) between a projectile ion and individual atoms of a target surface. The ion-surface scattering process at high energies forms the basis of conventional ion scattering spectroscopy (ISS), which performs elemental and structural analysis of surfaces.[54,55] On the other hand, at energies below ~100 eV, often called the hyperthremal energies, a projectile ion approaching a target surface sees the surface as a relatively smooth structure with insignificant atomic corrugation.[56] Thus, the BC approximation may no longer be valid for the low energy ion-surface collisions. Also, a projectile moves very slowly at a low energy. For example, a Cs^+ ion with a kinetic energy of 10 eV has a velocity of 3.8×10^3 m s^{-1}, which is of the order of the velocity of sound in typical solids. This implies that during the collision the surface atoms connected through the bonding network can respond collectively to the ion impact.[57] Consequently, many-body effects are important for the low energy ion-surface collisions. This causes a significant deviation from the BC behavior, with prominent multiple scattering events of low energy ions from the surface.

The evidence of multiple scattering events has been observed for the collisions of heavy projectile ions (Ar^+, Xe^+, and Cs^+) with a Si surface at low energies.[57,58] According to the ion-surface scattering kinematics of the BC model, a projectile heavier than a target atom cannot backscatter from a surface at arbitrary angles, and the scattering events should be confined to $\theta_{max} \leq \sin^{-1}(M_2/M_1)$ according to eq. (1).[54,55]

$$\frac{E_s}{E_i} = \frac{1}{(1+A)^2}[\cos\theta \pm (A^2 - \sin^2\theta)^{1/2}]^2 \qquad \text{(eq. 1)}$$

where E_s is the energy of the scattered projectile, E_i is the projectile incidence energy, $A = M_2/M_1$ with M_1 and M_2 being the projectile and target atom masses, respectively, and θ is the laboratory scattering angle. For example, θ_{max} is expected to be about 44° and 12° for Ar^+ and Xe^+, respectively, scattering from Si. Nevertheless, the experiments observe that these projectiles do scatter at much larger angles than θ_{max}.[57]

The kinetic energy distribution of reflected projectiles from a surface is also an important factor related to the RIS mechanism. Evstifeev and coworkers[59,60] observed that the energies of Cs^+ ions scattering from W, Mo, Co, and U surfaces were unusually higher than expected from sequential BCs with the surface atoms. Yang *et al.*[57] studied the scattering of 3 - 300 eV Cs^+ ions from Si in a 45°/45° scattering geometry and observed that the E_s/E_i ratio varied drastically with E_i. Figure 1 shows the observation that the E_s/E_i ratio for Cs^+ is initially very high (0.64 at E_i = 3 eV) and drops sharply to 0.1 as the energy increases to E_i > 100 eV. Such a large variation in E_s/E_i suggests that extensive multiple collisions take place at low incident energies. A notable feature is that even when the incidence energy increases substantially above 20 eV, the *absolute* E_s value remains fairly constant and low. As a result, the energy of scattered Cs^+ ions largely overlaps with the energies of sputtered particles.[2-4,61] This is important for the occurrence of the RIS process, as will be discussed in Section (2.2). One might question how many surface atoms actually make direct contact with a projectile during a low energy collision. Molecular dynamics (MD) simulations of Cs projectiles scattering from a Si surface show that only a few Si atoms experience direct collisions with the projectile.[57] The neighboring lattice atoms, however, collectively respond to the projectile impact through the bonding network of a solid. Such a dynamical effect causes an apparent increase in the effective mass of the surface, as shown in Fig. 1.

A large projectile/target mass ratio affects the angular dependency in the scattered particle flux distribution as well as in their E_s/E_i ratio. Heavy projectiles scatter preferentially with a narrow angular distribution towards a supraspecular direction.[56,61,62] The E_s/E_i ratio of an angle-resolved scattered flux increases as the scattering angle increases toward a glancing direction.[56]

Reactive Ion Scattering Mechanism. The RIS process of low energy Cs^+ is illustrated schematically in Fig. 2 by showing the trajectory of a Cs^+ ion colliding with a surface adsorbed with a molecule. A simple analogy of this process, which might be too simplified in rigorous scientific standards, is the action of a fisherman snatching a fish from water with a harpoon. A Cs^+ ion ("harpoon") picks up a molecule X ("fish") from water, leading to the formation of a CsX^+ ion complex ("speared fish"). CsX^+ is detected by a mass spectrometer and the mass of CsX^+ is measured ("weighing" a fish), thus identifying the molecule. Scientific explanation of the RIS mechanism is given in the following.

A typical result of RIS experiments for detecting surface molecules is shown in the mass spectrum of Fig. 3. In this study,[5] OH, CO, and d_6-benzene were coadsorbed on a Ni(111) surface and the surface was impacted with an incident Cs^+ beam at 30 eV. The spectrum is characterized by two kinds of peaks.

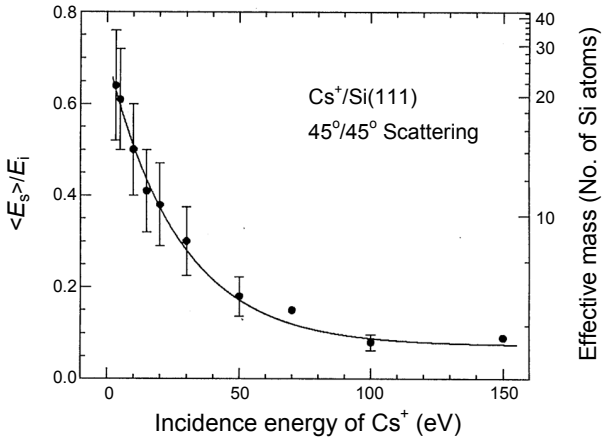

Figure 1. Ratio of the scattered to incident Cs^+ energy ($<E_s>/E_i$) as a function of E_i. The effective mass of a Si surface indicated on the right-hand side ordinate is deduced from the $<E_s>/E_i$ ratio and the BC model (Fig. 2 of Ref. 57).

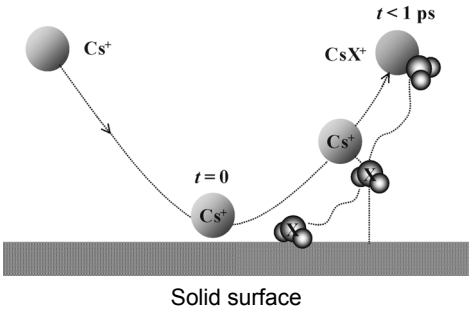

Figure 2. Pictorial illustration of the RIS trajectory leading to CsX^+ formation. Low energy collision of Cs^+ causes desorption of a neutral molecule X from the surface and formation of a transient CsX^+ complex *via* ion-molecule attraction forces between Cs^+ and X. The CsX^+ complex can be stabilized while CsX^+ stays close to the surface ($t < 10^{-12}$ s) which acts as a third body.

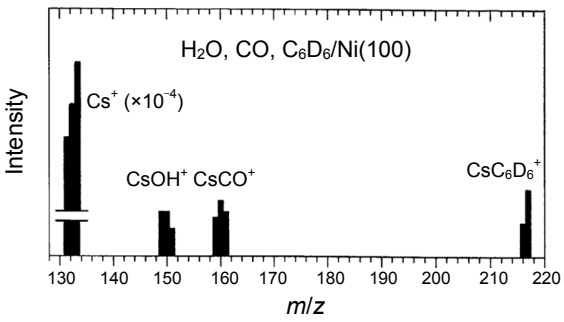

Figure 3. Mass spectra of the ions emitted upon 30 eV Cs^+ impact of a Ni(100) surface chemisorbed with OH, CO, and d_6-benzene (Fig. 3 of Ref. 6).

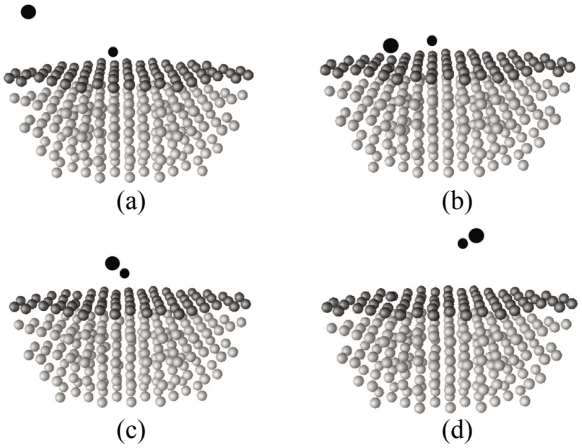

Figure 4. Illustration of the RIS abstraction mechanism in four snapshots of a trajectory of Cs^+ scattering from a Pt(111) substrate surface: a) initial positions before impact; b) impact of the Cs^+ and energy release to the surface; c) the Cs^+ pulling the adsorbate away in its outgoing trajectory; and d) the slow outgoing Cs^+ dragging the adsorbate along with, both particles scattering as a Cs^+-adsorbate RIS product (Fig. 4 of Ref. 50).

(i) A Cs^+ peak that is elastically (non-reactively) scattered from a surface appears at m/z = 133 *amu/charge*. (ii) Peaks above m/z = 133 *amu/charge* represent RIS signals due to the pickup of surface molecules by Cs^+. The RIS signals include $CsOH^+$ (m/z = 150), $CsCO^+$ (m/z = 161), and $CsC_6D_6^+$ (m/z = 217). These signals indicate that all the surface molecules are detected without fragmentation of the molecules. The OH adsorbate is produced *via* dissociative chemisorption of H_2O on the Ni surface, rather than *via* collisional fragmentation of H_2O molecule.[6] A $CsNi^+$ signal is absent from the surface, indicating that sputtering of Ni atoms is negligible at a collision energy of 30 eV. The peak intensity ratio of CsX^+/Cs^+ indicates the efficiency of molecule pickup by Cs^+, which is defined as the RIS yield, Y(X). This ratio is of the order of 10^{-4}, which is a typical value for chemisorbed molecules on surfaces. Y(X) can be as high as 0.1 - 1 for weakly physisorbed molecules, as will be discussed shortly. Note that these Y(X) values are 10^2 - 10^6 times greater than the ionization efficiency ($\sim 10^{-6}$) of gas molecules inside an electron impact ionizer of a mass spectrometer. This indicates that the RIS process converts neutral adsorbates (X) into gaseous ions (CsX^+) with much higher efficiency than other desorption-based surface analysis methods do, including thermal desorption mass spectrometry, laser ablation mass spectrometry, and secondary ion mass spectrometry. Thus, RIS can detect surface molecules with high sensitivity.

The mechanism of the RIS process has been investigated by Kang and coworkers.[4-6,48-51] In the early RIS experiments with chemisorbed species, where very small RIS yields ($\sim 10^{-4}$) were observed, the RIS processes were considered to occur *via* a two-step mechanism; the Cs^+ impact causes collision-induced desorption (CID) of adsorbates and the Cs^+-molecule association occurs in the outgoing trajectory.[4-6] However, in the later experiments, much higher (up to ~1) RIS yields were observed for small molecules physisorbed on surfaces, such as CO_2, H_2O, and noble gases on metal surfaces[51-53] and frozen water films.[8,12-15,32] The early two-step mechanism cannot explain the high RIS yields observed in these experiments. Studies using classical molecular dynamics simulations[48-50] support the idea that the RIS process actually occurs *via* a one-step abstraction mechanism, which is categorized as an Eley-Rideal (ER) type surface reaction. Figure 4 illustrates this one-step abstraction mechanism with four representative snapshots of the simulated RIS trajectory. The abstraction reaction is driven by the ion-dipole attraction force between a Cs^+ ion and an adsorbate molecule. The ion-dipole attraction induces desorption of the adsorbate which is the precursor to the formation of a Cs^+-adsorbate product. The impinging projectile at first releases part of its initial energy to the surface (Fig. 4b), even without directly colliding with the adsorbate, and subsequently pulls the adsorbate gently away from the surface in the outgoing trajectory (Figs. 4c and 4d in sequence). The velocity of the outgoing Cs^+ must be slow enough to accommodate for the adsorbate's inertia. As a result, adsorbates of low mass are efficiently abstracted. Also, a heavier projectile transfers more energy to the target surface, and the lower velocity in the outgoing trajectory enhances the RIS efficiency. This explains the experimental observations that Cs^+ is the most effective projectile in forming the RIS products among various alkali metal ions.[4]

Figure 5 shows the result of the statistical analysis of the scattering events of Cs^+ projectiles from a Pt(111) surface with a physisorbed adsorbate of 16 *amu* mass.[50] The adsorbate binding energy to the surface is E_b = 0.25 (top), 0.5 (middle), and 1.0 eV (bottom). Two processes are responsible for the removal of the adsorbates from the surface: collision-induced desorp-

tion of adsorbates and the direct abstraction by Cs^+ (RIS process). Their relative efficiencies are shown in the figure by plotting their cross-sections as a function of Cs^+ incidence energy. The CID cross-sections (solid symbols) exhibit the well-known energy dependence: a monotonic increase with Cs^+ energy, steep at the beginning with gradual saturation. On the other hand, the RIS cross-sections (gray areas) due to the ion-dipole attraction show very different energy dependences. For E_b = 0.25 eV (physisorbed species), the RIS cross-section is larger than the CID cross-section at the low energy side and exhibits a maximum at around E_i = 10 eV. The RIS cross-section decreases as E_b increases. For E_b = 1.0 eV (chemisorbed species), the adsorbates are desorbed mostly *via* a CID process without CsX^+ formation, and the RIS process occurs only with very small efficiency. Such different behaviors with the magnitude of E_b explain why the RIS process occurs much more efficiently for physisorbed species with a smaller binding energy to the surface than for strongly chemisorbed species.

Ion-surface collisions at low energies (< 100 eV) mainly desorb neutral species from surfaces. This is because the yield for secondary particle ionization is very small or negligible at low energies, a situation different from the keV ion-surface collisions employed in secondary ion mass spectrometry experiments. However, when preformed ions exist on a surface, these ions can be ejected even by the low-energy ion impact. This type of process can occur for systems such as alkali metal ions on a high work-function surface[63] and electrolyte ions that are stabilized by water solvation on an ice surface.[8,12-15,32] The collisional desorption of preexisting ions, called the low energy sputtering (LES), has been investigated in the author's group on various ion-containing surfaces.[8,12-15,32,63] Figure 6 shows the result of LES study for hydronium (H_3O^+) and ammonium ions (NH_4^+) on ice film surfaces at a low temperature.[14] These ions are prepared on the ice surface by the adsorption and ionization of HCl and subsequent acid-base reactions between H_3O^+ and adsorbed NH_3. The figure shows LES intensities of these ions as a function of Cs^+ impact energy. NH_4^+ and H_3O^+ are emitted at the energies above 17 and 19 eV, respectively, from the ice surface containing both preformed NH_4^+ and H_3O^+ ions. On a pure H_2O or NH_3 surface, on which no H_3O^+ or NH_4^+ exists, the thresholds for H_3O^+ and NH_4^+ emission appear at much higher energies (≥ 60 eV). Evidently, a large gap in the threshold energies exists for ejecting the same ions from two different surfaces, the one containing the preformed ions and the other having only neutral molecules. In the latter, the NH_4^+ and H_3O^+ signals must be produced by secondary ionization processes, which require a significantly larger energy than the LES of preexisting ions. These preformed ions can be ejected without significant fragmentation of their molecular structures, if Cs^+ impact energy is carefully controlled near the threshold energy. Therefore, LES can be used to identify molecular ions on surfaces.

In practice, we can simultaneously record the LES signals of ion desorption (Y^+) and the RIS signals (CsX^+) in one mass spectrum. The RIS signals appear at the higher masses than Cs^+ (m/z = 133), while the LES signals for small ions appear at low masses. Therefore, the LES and RIS signals are well distinguished in the mass spectrum in most experiments. The combined use of LES and RIS experiments is a powerful method to detect both neutral (X) and ionic species (Y^+) on a surface.

Experimental Apparatus, Operation Modes, and Quantification. The instrumentation for RIS experiments includes a low-energy Cs^+ gun, a mass spectrometer with the ability of ion-pulse counting, a sample mounting stage, and a vacuum chamber. Only a brief description of the instrumentation is given here; more details can be found elsewhere.[6,16] Figure 7 shows a schematic drawing for an instrument equipped with a quadrupole mass spectrometer (QMS) and a rotatable Cs^+ ion gun. The ion gun (Kimball Physics) provides a Cs^+ beam at energies 1 - 100 eV. The Cs^+ beam current density at a target is con-

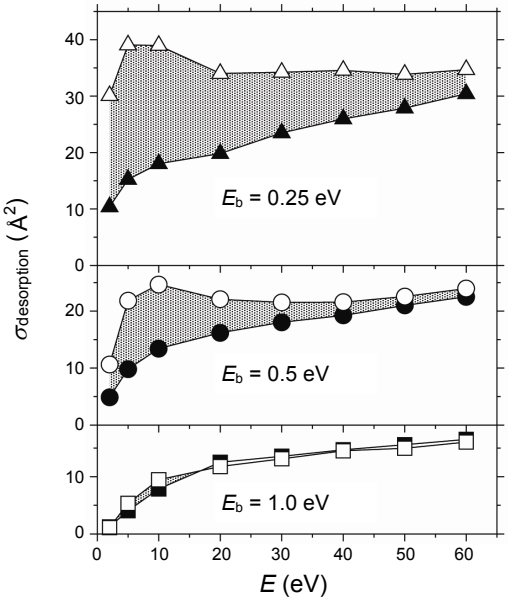

Figure 5. The overall desorption (empty symbols) and CID (solid symbols) cross-sections as function of the Cs^+ incidence energy (E_i) for three adsorbate binding energies (E_b).The CID cross-sections are deduced from simulations without ion-dipole attraction. The gray areas mark the enhancement due to desorption by the ion-dipole attraction, or the RIS process. The Cs^+ incidence angle is 45° and the adsorbate mass is 16 amu (Fig. 1 of Ref. 50).

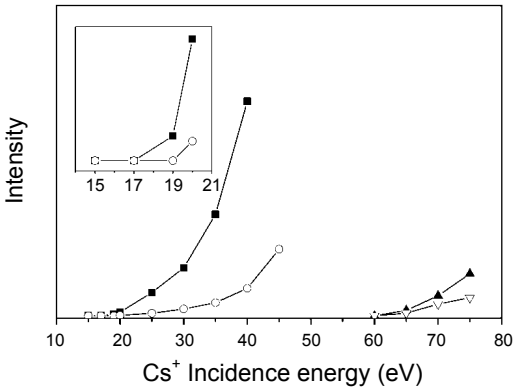

Figure 6. The intensity of hydronium and ammonium ions emitted from two different types of surfaces as a function of collision energy. For a surface prepared by co-exposure of 0.3 L (1 Langmuir = 1×10^{-6} Torr s) HCl and 0.15 L NH_3 on a D_2O-ice layer at 100 K, ammonium (■) and hydronium (○) ions are emitted at energies above 17 and 19 eV, respectively. The inset magnifies the threshold region. On frozen films of pure D_2O or NH_3, the thresholds for hydronium (▲) and ammonium (▽) ions are much higher (~60 eV) (Fig. 3 of Ref. 14).

trolled to be typically ~1 nA cm^{-2}. A higher beam current increases the sensitivity of RIS analysis, but at the same time, the target surface is contaminated more quickly due to Cs^+ deposition from the beam, and the surface is more severely damaged by the ion impact. The QMS is operated in an ion detection mode with its ionizer switched off, since LES and RIS signals are all ions. This has a clear advantage that the signals are measured with almost zero background noise, if the sources of stray ions inside a vacuum chamber are removed. In the instrument shown in Fig. 7, the angle of ion incidence to a target surface and the detector angle can be varied by independent rotary motions of the Cs^+ gun and the sample mounting stage. For the purpose of surface analysis only, however, an instrument with a fixed scattering angle is sufficient. In this case, optimal RIS conditions for surface analysis can be found for a specular scattering geometry at the angle between 90° - 120° (45° - 60° for both incident beam and detector angles with respect to the surface normal), according to the results of angle-resolved RIS studies[6,16] and MD simulations.[50]

RIS experiments can be performed in several different modes of operation depending on the information desired. First, for the purpose of surface analysis and molecular identification, a mass spectrum of RIS signals is obtained from a sample by scanning a QMS in an appropriate mass range. In addition, LES signals may be simultaneously recorded with the RIS signals to obtain the information about ionic adsorbates, as mentioned above. In most experiments, the RIS signals are well separable from the LES signals at low masses because the former appears at masses above m/z = 133.

Second, for a study of surface reaction kinetics, the population change of surface adsorbates is measured as a function of time. The changes for several adsorbates can simultaneously be monitored by using the multiple ion-detection mode of a mass spectrometer, a feature now available in many QMS instruments. For instance, a QMS is tuned to the masses of pre-selected species of interest which correspond to reactants, intermediates, and products of the reaction under the investigation, and their intensity variations are measured in real time.[6] An RIS instrument employing a continuous Cs^+ beam current of

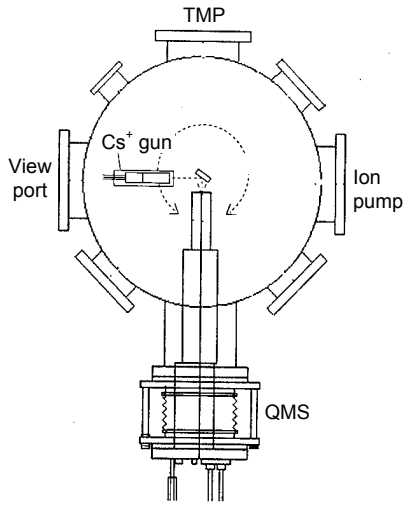

Figure 7. An angle-resolved RIS chamber equipped with a QMS and a rotatable Cs^+ ion gun (top view) (Fig. 2 of Ref. 16).

~1 nA cm^{-2} can give a signal intensity that is strong enough to perform the real-time kinetic measurement with a temporal resolution of ~1 s. Of course, the RIS signal intensity and the speed of the kinetic measurement depend on the detection efficiency of the adsorbates being investigated. The performance of RIS for a kinetic measurement in terms of the temporal resolution is comparable to or better than that of the currently most sensitive tools of surface analysis, including Auger electron spectroscopy. A prolonged exposure of a Cs^+ beam onto a sample surface can lead to surface contamination, but this effect may be negligible for a measurement time up to ~100 s when the beam current density is ~1 nA cm^{-2}.

Third, a temperature-programmed RIS (TP-RIS) experiment is performed to study the temperature-dependence of surface reactions. In this experiment the sample temperature is varied in a controlled way, similar to that used in a temperature-programmed desorption (TPD) experiment. The difference is that while TPD detects desorbing species from a surface, TP-RIS measures surface species. TP-RIS monitors the population changes of adsorbates as a function of temperature and their conversion *via* surface reactions. Since the temperature of a sample can be varied over a wide range in surface science experiments, and the speed of reaction varies with sensitive correspondence to the surface temperature, TP-RIS provides a powerful method for the study of kinetics and mechanisms of surface reactions.[17,18,64] In particular, reaction intermediates can be trapped on a surface at a cryogenic temperature and be identified with RIS.[23-26,42-44]

Quantitative measurement of surface adsorbates is an important goal in surface analysis. In the following, a relationship between the surface coverage of adsorbates and their RIS signal intensity is discussed. In an ideal situation, RIS signal intensity is expected to be proportional to the flux of an incident Cs^+ beam and the amount of adsorbate on the surface. To quantitate this relationship, we define the RIS yield, Y(X), as the intensity ratio of CsX^+ to all scattered ions including Cs^+ and RIS products (eq. 2).

$$Y(\mathrm{X}) = \frac{I(\mathrm{CsX}^+)}{I(\mathrm{Cs}^+) + \sum I(\mathrm{CsX}^+)} \qquad \text{(eq. 2)}$$

where $I(CsX^+)$ is the signal intensity of CsX^+. Y(X) indicates the RIS abstraction efficiency of adsorbates (X) from the surface, and its value is calculated from an RIS spectrum. Y(X) depends on the adsorbate surface coverage (θ). A measure of the RIS efficiency that is independent of θ is the RIS cross-section (σ_{RIS}), defined by eq. (3).

$$\sigma_{\mathrm{RIS}} = \left.\frac{\mathrm{d}Y}{\mathrm{d}\theta}\right|_{\theta<0.1\mathrm{ML}} \qquad \text{(eq. 3)}$$

σ_{RIS} is obtained from the slope of an RIS yield curve measured as a function of θ. This procedure has been described for noble gases, CO, CO_2, and H_2O adsorbed on metal surfaces.[51,53] σ_{RIS} represents the effective area (Å^2) on the surface within which the RIS product can be formed upon the collision of a Cs^+ projectile. Equation (3) is valid for isolated adsorbates on a surface in the absence of multiple ion impacts on the same surface

spot, i.e., the relationship holds for a low adsorbate coverage and a low beam flux. These conditions are satisfied typically for $\theta \leq 0.1$ ML and a Cs^+ dose ≤ 0.02 ions $Å^{-2}$. In this regime, the RIS parameters [$I(CsX^+)$, $Y(X)$, and $\theta(X)$] all exhibit a mutual linear dependency. Thus, $\theta(X)$ can be deduced from RIS intensities in a semi-quantitative manner.

Determination of the *absolute* value of $\theta(X)$ requires a calibration experiment be done with a reference sample which has a known quantity of adsorbate. This is because the RIS cross-section is specific to an adsorbate, and it varies sensitively with the adsorbate nature such as its dipole moment and surface binding energy, as discussed in Section 2.2. Once σ_{RIS} is obtained from the calibration experiment, then quantitative determination of $\theta(X)$ for the adsorbate is possible. If several adsorbates coexist on a surface, a separate calibration experiment for each species will be able to achieve quantitative analysis of the co-adsorbed species.

The sensitivity of RIS for detecting adsorbates, in terms of the amount of adsorbate coverage, is typically a few percent of monolayer for chemisorbed species like CO on Ni, when the spectrum is acquired by using a Cs^+ beam current of ~1 nA cm^{-2} for a duration of ~1 min.[6] The RIS detection sensitivity for physisorbed species can be higher because they exhibit higher RIS yields (0.1 - 1) than that for chemisorbed species ($\sim 10^{-4}$).

Cs^+ beam energy is an important control variable in RIS experiments. It affects the RIS detection sensitivity as well as the degree of fragmentation of molecular adsorbates. One can extract some information about the structure of molecular adsorbates from examination of the effect of ion impact energy on RIS signal intensity and the pattern of molecular adsorbate fragmentation.[17]

Applications

Catalytic Reactions on Surfaces. The ability of RIS for detecting molecules on surfaces with high sensitivity makes this technique a powerful tool to study the kinetics of heterogeneous catalytic reactions. As such, RIS studies have been performed for adsorption and desorption kinetics of molecules,[5,6] clustering reactions of Cs adatoms on Si,[9] decomposition of organosilanes on Si,[10,11] dehydrogenation and H/D exchange reactions of ethylene on Pt,[17,18] catalytic oxidation of CO on Pt,[23] and the proton exchange between water and cysteine molecular films on Au.[64]

An example of a study of surface reactions to be described here in more detail is the H/D exchange reaction of ethylene (CH_2=CH_2) with hydrogen on Pt(111).[18] This is one of the model reactions of heterogeneous catalysis, and the reaction mechanism has been a subject of extensive studies by using a variety of surface spectroscopic techniques.[65,66] The H/D exchange mechanism is a key to understanding for the catalytic hydrogenation and dehydrogenation of ethylene.[67] Figure 8 shows the result of a RIS study for H/D isotopic exchange reactions between C_2D_4 and H on a Pt(111) surface.[18] In this experiment, the Pt(111) surface is coadsorbed with H and C_2D_4 at two different temperatures: (a) 200 K, at which H/D exchange is prohibited and (b) 270 K, at which H/D exchange is activated. Spectrum (a) verifies that ethylene adsorbs on Pt(111) in a molecular state without dissociation or H/D exchange reactions at 200 K. Spectrum (b) shows various ethylene isotopomers (C_2D_3H, $C_2D_2H_2$, C_2DH_3, and C_2H_4) resulting from the occurrence of H/D exchange reactions at 270 K. Note that the intensity distribution in spectrum (b) truly represents the relative amounts of ethylene isotopomers present on the surface. In the absence of the ionizer function of the mass spectrometer, the possibility of molecular cracking and isotopic scrambling during the measurement can be eliminated. Also, the ethylene isotopomers with similar geometric structures should exhibit almost the same detection efficiency for RIS.

TP-RIS measurements for the $C_2D_{4-x}H_x$ (x = 0 - 3) species reveal temperature dependency of the H/D exchange reactions. The TP-RIS result shown in Fig. 9, obtained during a temperature scan from 230 K to 295 K, indicates that the H/D exchange reaction takes place even below 230 K. The curves also show that the accumulation of C_2D_3H is necessary to form $C_2D_2H_2$, and it is the same for the formation of C_2DH_3. Therefore, the H/D exchange reaction takes place sequentially. The intensity of C_2D_4 decreases sharply at temperatures higher than 265 K, and all of the ethylene species disappear completely when temperature reaches 290 K. The depletion of ethylene on the surface is due to the dehydrogenation of ethylene to ethylidyne (CH_3-C≡), a path observed in the previous studies of thermal decomposition of ethylene.[17,67]

The kinetic curves in Fig. 9 indicate that the H/D-exchange reaction rate increases abruptly when the surface temperature reaches ~260 K. This peculiar feature evokes an interpretation that a different reaction channel becomes operative at this temperature. Based on these kinetic observations and the information available in the literature, Kim *et al.*[18] propose a mechanism for the H/D exchange reaction of ethylene on Pt(111), which is summarized in the scheme drawn in Fig. 10. At temperatures lower than 260 K, the reaction proceeds *via* ethyl intermediate (CH_3-CH_2-; path a), which is consistent with a previously proposed mechanism.[65,66] When the surface temperature reaches 265 K, however, ethylidene species (CH_3-CH=)

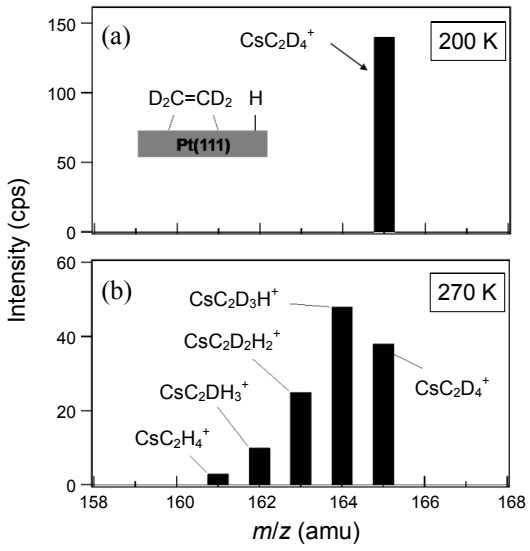

Figure 8. RIS mass spectra from a Pt(111) surface dosed with 5 L of H_2 and 0.5 L of C_2D_4 at 200 K. The sample temperature is 200 K (a) and 270 K (b) (Fig. 1 of Ref. 18).

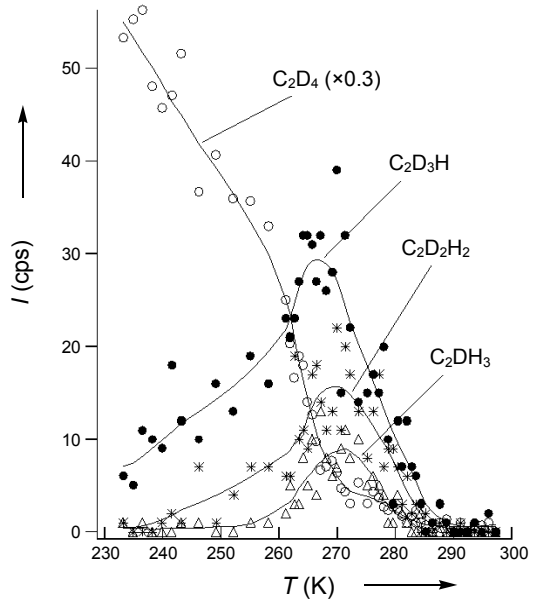

Figure 9. Real-time monitoring of the signal intensity variations for C_2D_4 (○), C_2D_3H (●), $C_2D_2H_2$ (*), and C_2DH_3 (Δ) on Pt(111) during a temperature increase. The sample surface is prepared by doing 5 L of H_2 followed by 0.5 L of C_2D_4 at 200 K. The heating rate is 0.3 K s^{-1}. Lines are drawn to aid the eye (Fig. 2 of Ref. 18).

is formed on the surface, and C_2D_3H is produced alternatively by α-hydrogen exchange (path b). This new channel signifies the role of surface ethylidene species in the H/D exchange reaction and, therefore, in the hydrogenation and dehydrogenation of ethylene as well. Ethylidene finally decomposes to ethylidyne at higher temperatures.

As the above example shows, RIS can identify H/D-substituted ethylene isotopomers existing on the surface and measure their relative populations during the H/D exchange reaction as a function of temperature. RIS is ideally suited for a study of surface reaction kinetics and mechanisms especially when similar molecules are involved. Considering that quantitative determination of multiple H/D-substituted molecules is a difficult task in surface analysis, RIS has unique ability for this application.

Physisorbed Molecules: Chemistry of Ice Surfaces. RIS shows the highest detection sensitivity for weakly physisorbed molecules. For example, the RIS yield for picking up a water molecule from an ice film surface can reach almost ~1.[8] This feature makes a frozen molecular film grown on a cold substrate, such as a water-ice film, particularly an attractive system to study with RIS. On ice films, however, only a small portion of incident Cs^+ projectiles are reflected from the surface without penetration owing to the soft structure of the surface, and this reduces the scattered Cs^+ intensity.[48b] Despite such inefficient backscattering of Cs^+ projectiles, the resulting RIS product signals can be quite strong on the ice films, because the high RIS yields for physisorbed species compensate the reduced Cs^+ intensity. An ice film sometimes contains preformed ionic species, which are stabilized on the surface through water solvation. A good example is strong electrolytes ionized on ice films.[12-15,32] These preexisting ions can be detected by means of LES. A combined usage of two methods allows one to detect both neutral

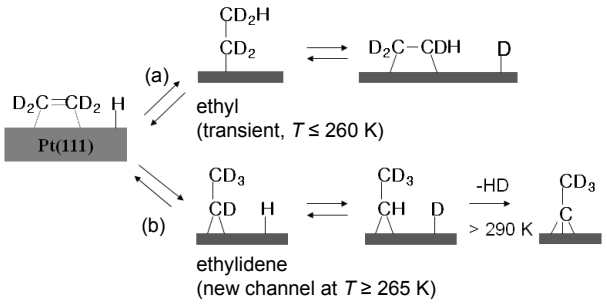

Figure 10. Reaction mechanisms for the H/D exchange reaction of ethylene on Pt(111).

molecules and ions on the surface and, therefore, to investigate the ionization process of electrolytes on the surfaces. Studies in this line of research have greatly contributed to understanding of physics and chemistry of ice surfaces in the past decade. They include the RIS and LES studies of surface diffusion of water molecules,[28] ionization of electrolytes,[29-31] acid-base chemistry,[12,32-35] proton transfer,[36-41] and various types of reactions that are either of fundamental interest[42-44] or related to environmental chemistry[25-26] and astrochemistry.[45,46] These subjects have been reviewed recently.[27,47]

Ice surfaces offer a unique reaction environment, which is quite different from a liquid water or gas environment. Until recently, the study of reactions on ice surfaces at low temperatures has been very limited compared to that of aqueous or gas phase reactions. The most extensively studied example of ice surface reaction is the ionization of strong protic acids such as HCl, for which reviews are available.[68] The author's group has examined the adsorption and ionization of HCl on ice films at low temperatures (50 - 140 K) with RIS and LES.[12,34] Figure 11(a) shows the RIS spectrum obtained from a D_2O-ice film surface with HCl adsorbates (~0.3 ML) at a temperature of 70 K. A family of $Cs(D_2O)_n^+$ (n = 1 - 4) peaks appear in the spectrum, along with a $CsHCl^+$ peak. The $CsHCl^+$ signal indicates that HCl exists as an undissociated molecule on the surface at this temperature. In Fig. 11(b), obtained at 140 K, the $CsHCl^+$ peak disappears, though the $Cs(D_2O)_n^+$ clusters remain. This suggests the transformation of molecular HCl at 70 K to an ionized form at 140 K.

Figure 12 presents the LES spectra taken after HCl adsorption on an ice film at 110 K. In the LES spectrum of positive ions shown in Fig.12(a), hydronium ions (D_3O^+, HD_2O^+, and H_2DO^+) are detected at m/z = 20 - 22 along with their hydrated clusters at m/z = 39 - 42. In the negative ion LES spectrum (Fig. 12b), Cl^- (m/z = 35 and 37) and its hydrated ions are detected. These LES signals clearly support the ionization of HCl molecules into hydronium and chloride ions at 110 K. The hydronium ion signals appear above an apparent threshold energy of 10 - 12 eV on the HCl-adsorbed ice surface, whereas they appear only at much higher energies (> 60 eV) on a pure ice film due to secondary ionization of water molecules.[33] In addition, the intensities of hydronium and chloride ion signals decrease when HCl is adsorbed at a reduced temperature. Therefore, these ion signals must originate from the ionized HCl on the surface. The observed various H/D-isotopomers of hydronium ions indicate that they undergo facile H/D exchange reactions with

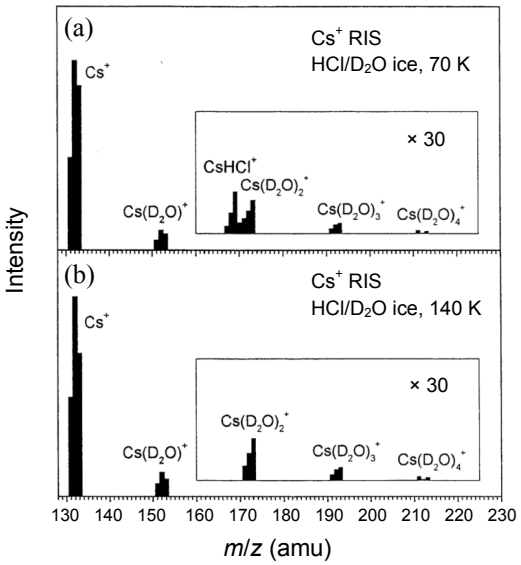

Figure 11. RIS mass spectra measured after exposing HCl onto a D_2O-ice film for 0.3 L. (a) HCl exposure temperature of 70 K and (b) 140 K. Cs^+ impact energy is 20 eV. The spectra are displayed in low mass resolution (Fig. 1 of Ref. 12).

surface water molecules.

The signal intensities of $CsHCl^+$ and hydronium ion are measured as a function of the ice temperature over 50 - 140 K.[12] Figure 13 summarizes the result, showing the relative portion of HCl molecules and hydronium ions on the ice surface at various temperatures. The ionized HCl has only a small population at 50 K, but its portion increases with temperature toward complete ionization at 140 K. The crossing point of the molecular and ionized HCl curves occurs at about 110 K. The results point out some interesting properties of HCl on ice. Although HCl is a strong acid and completely ionizes in an aqueous solution at room temperature, it exists both in molecular and ionized states on ice at low temperatures. Therefore, HCl acts as a weak acid under these conditions, the relative portions of the molecular and ionized states varying with the temperature as shown in the figure. Also, the study suggests that HCl ionizes completely on ice particles in the polar stratospheric clouds (PSCs, $T > 200$ K). In this context, HCl will contribute to the ozone depletion processes in PSCs *via* ionic reaction mechanisms.[69]

An interesting aspect in the study of reactions on ice surfaces is that the reaction speed can be slowed down by cooling the sample, and sometimes the reaction intermediates can be kinetically isolated on the surface to be identified by spectroscopic methods. These are clear advantages over studying reactions in liquid water or at a gas/water interface, where it is often difficult to detect the reaction intermediates due to their transient lifetimes. The reaction of SO_2 will be presented as an example of a study of reactions on ice surfaces. SO_2 is an atmospherically important trace gas. Kim *et al.*[25] studied the adsorption of SO_2 on ice films and subsequent reactions at temperatures above 80 K. RIS and LES were used to monitor the reaction on the surface, in conjunction with TPD to monitor the desorbing species. Figure 14 shows the results of RIS and LES measurements on an ice film with SO_2 adsorbates at 140 K. Spectrum (a) shows that the RIS signals related to SO_2 adsorbates are

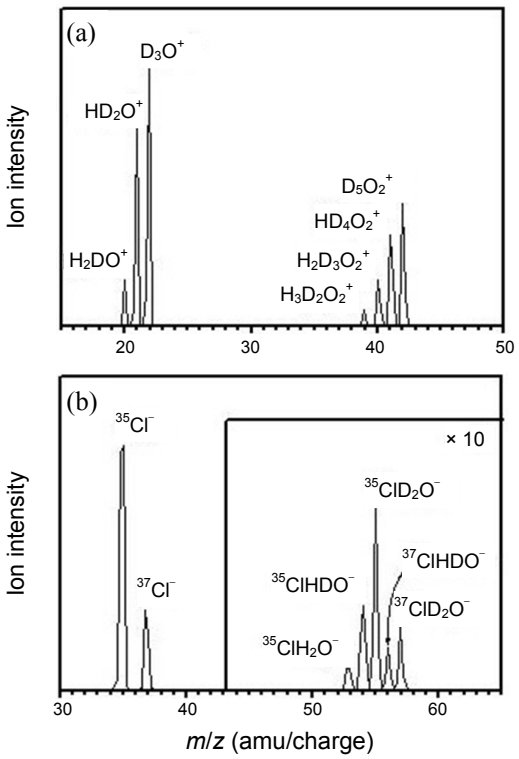

Figure 12. LES mass spectra of positive (a) and negative ions (b) obtained on a HCl/D_2O-ice film prepared by HCl exposure of 0.5 L at 110 K. The Cs^+ beam energy is higher (50 eV) than in usual LES experiments to increase the signal intensity. The ice film is grown on Ru(0001).

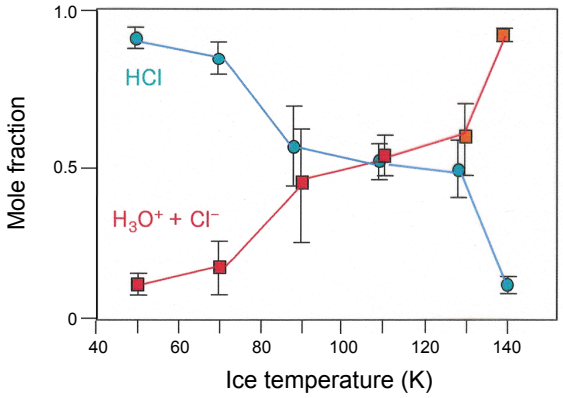

Figure 13. Relative portions of molecular HCl (●) and hydronium ion (■) present on a HCl/D_2O-ice film at various temperatures. HCl exposure is 0.3 L (Fig. 3 of Ref. 12).

$CsSO_2^+$ ($m/z = 197$), $CsDSO_2^+$ ($m/z = 199$), and $Cs(D_2O)(SO_2)^+$ ($m/z = 217$). The $CsSO_2^+$ and $Cs(D_2O)(SO_2)^+$ peaks indicate the presence of molecular SO_2 adsorbates. Noticeably, the $CsDSO_2^+$ peak indicates the formation of DSO_2 species. Spectrum (b) shows LES anion signals from the surface, which include OD^- ($m/z = 18$), SO_2^- ($m/z = 64$), DSO_2^- ($m/z = 66$), and DSO_3^- ($m/z = 82$). These signals indicate that SO_2 is transformed into various molecular anions by hydrolysis on the ice surface. In contrast, the positive-ion LES spectrum (Spectrum c) does not show any cation related to SO_2 adsorbates. The small Na^+, K^+, and Rb^+ peaks are due to alkali ion impurities in the

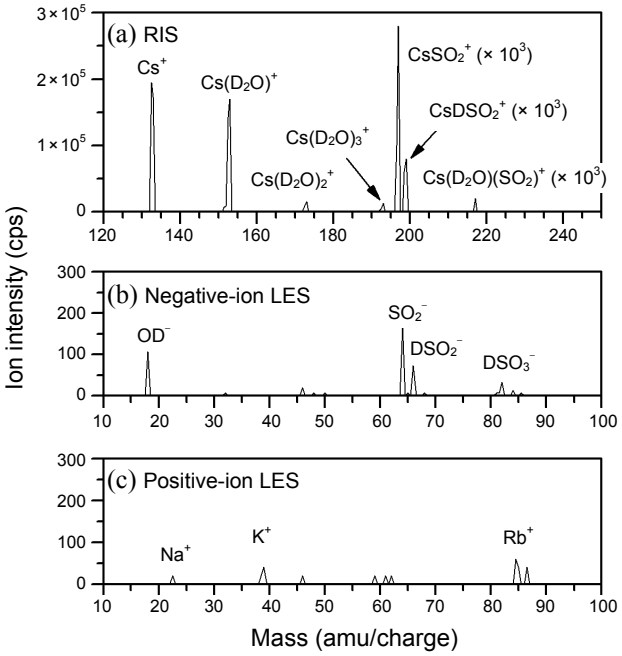

Figure 14. (a) RIS mass spectrum obtained from a D_2O-ice film exposed to SO_2. (b) LES spectrum of negative ions. (c) LES spectrum of positive ions. The ice film (4 bilayer thickness) is exposed to SO_2 for 0.2 L at 80 K, and the RIS and LES measurements are made at 140 K. The RIS signals at masses above m/z = 190 amu/charge are magnified by the factors indicated (Fig. 1 of Ref. 25).

Cs^+ beam.

When an ice film adsorbed with SO_2 is warmed slowly from 80 - 150 K, the signals of various SO_2-related species appear and disappear at different temperatures. The result is shown by TP-RIS and TP-LES curves in Fig. 15. Combined together, TP-RIS, TP-LES, and TPD observations indicate that the adsorption of SO_2 on ice produces three surfaces species: a solvated SO_2 species with a partial negative charge, a HSO_2 species, and an anionic HSO_3-like species.[47] Because these species are efficiently formed even at the low temperatures, the hydrolysis of SO_2 must occur with very small or negligible energy barriers. Also, these species may correspond to distinct intermediate stages in the hydrolysis mechanism, because they are trapped on the ice surface *via* kinetic isolation at the low temperatures. Such information may be useful for understanding the hydrolysis of SO_2 at gas/liquid interfaces as well, in particular, the nature of transient surface complexes formed at the interfaces.

The above examples demonstrate that RIS and LES can be used to reveal the chemical states of neutral molecules and ions present on ice surfaces and to measure their relative populations. At a low temperature, it is possible to isolate the reaction intermediates on the ice surfaces and take its "frozen snapshot". With these features, RIS and LES are expected to be a versatile and powerful tool for exploring the chemistry of ice surfaces.

Summary

RIS and LES techniques using low energy Cs^+ beams are relatively new, but they have already demonstrated that they have many promising applications in surface science research.

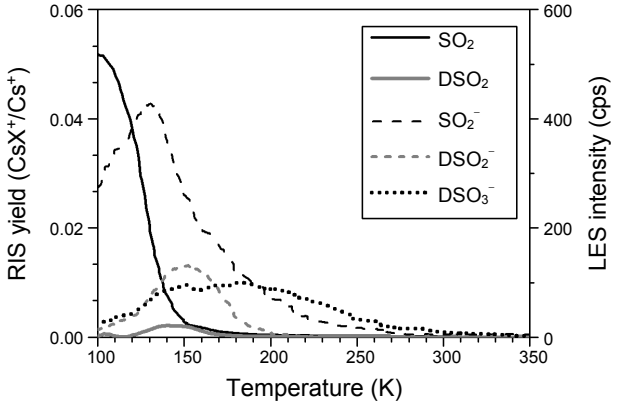

Figure 15. Temperature-programmed RIS and LES measurements for signals of interest detected on the surface of a D_2O-ice film adsorbed with SO_2. The left ordinate indicates the RIS yield for neutral species (SO_2 and DSO_2). The LES signals observed include SO_2^-, DSO_2^-, and DSO_3^-. SO_2 gas is adsorbed onto the surface at 80 K for 0.3 L. The temperature ramping rate is 1 K s^{-1} (Fig. 7 of Ref. 47).

The ability of RIS to identify molecules on surfaces is difficult for other surface spectroscopic methods developed to date to compete with. The unique features of RIS and LES can be summarized as follows.

(1) The RIS process occurs *via* Eley-Rideal type abstraction reactions. Owing to the purely physical nature of the ion-dipole attraction force between Cs^+ ions and adsorbed molecules, the RIS method can be universally applied to various molecular adsorbates. Moreover, the ultrafast (< 1 ps) nature of the RIS process improves the molecular detection ability by reducing the interference effects of slow molecular dissociation and secondary reactions on the surface.

(2) RIS can detect neutral molecules on surfaces with a high degree of sensitivity. The efficiency of RIS for converting neutral adsorbates (X) into gaseous ions (CsX^+) is ~10^{-4} for chemisorbed species and ~0.1 for physisorbed species, which exceeds the molecule ionization efficiency in TPD, laser ablation mass spectrometry, and secondary ion mass spectrometry.

(3) LES detects preexisting ions on surfaces. In LES, the possibility of secondary reactions due to ion impact can be minimized by employing a Cs^+ impact energy slightly above the sputtering threshold. The combined usage of RIS and LES methods allows one to analyze both neutral species and ions on the surface.

(4) RIS and LES are sensitive to the first monolayer of a surface because the low-energy ion impact ejects atoms and molecules exclusively from the top layer.

(5) RIS can quantitatively determine the relative amounts of isotopomer molecules without isotopic scrambling during the measurement.

(6) The kinetics of surface reactions can be monitored in real-time with a time resolution of ~1 s. TP-RIS and TP-LES experiments are useful for studying reaction intermediates and mechanisms.

On the other hand, there are some drawbacks of the techniques and features that need to be improved on:

(1) Quantitative surface analysis is difficult when several different adsorbates are involved, because the RIS yield varies widely depending on the nature of adsorbate. A calibration ex-

periment is necessary for each adsorbate species.

(2) RIS cannot determine the mass of very strongly adsorbed molecules that undergo molecular fragmentation rather than intact desorption upon Cs^+ impact. It is possible, however, to identify the end functional groups of these adsorbates.

(3) RIS is not effective for covalently bonded soft materials such as organic polymers and a self-assembled monolayer of long chain molecules, because these molecules are difficult to detach intact. In addition, Cs^+ projectiles do not efficiently backscatter on a soft surface.

Acknowledgments. I am grateful to my students and postdoctoral associates as well as the visiting scientists in my laboratory, who have contributed to the discovery, development, and application of RIS over the past 15 years. Part of the research efforts was supported by the National Research Foundation grant funded by the Korea government (MEST) (2010-0001638).

References

1. Ertl, G.; Küppers, J. *Low Energy Electrons and Surface Chemistry*; VCH Publishers: 1985.
2. Yang, M. C.; Lee, H. W.; Kang, H. *J. Chem. Phys*.**1995**, *103*, 5149.
3. Yang, M. C.; Hwang, C. H.; Ku, J. K.; Kang, H. *Surface Sci.* **1996**, *366*, L719.
4. Yang, M. C.; Hwang, C. H.; Kang, H. *J. Chem. Phys*. **1997**, *107*, 2611.
5. Kang, H.; Kim, K. D.; Kim, K. Y. *J. Am. Chem. Soc.* **1997**, *119*, 12002.
6. Kang, H.; Yang, M. C.; Kim, K. D.; Kim, K. Y. *Int. J. Mass Spectrom. Ion Proc*. **1998**, *174*, 143.
7. Kim, K.-Y.; Shin, T.-H.; Han, S.-J.; Kang, H. *Phys. Rev. Lett.* **1999**, *82*, 1329.
8. Shin, T.-H.; Han, S.-J.; Kang, H. *Nucl. Instrum. Methods in Phys. Res. B* **1999**, *157*, 191.
9. Han, S-J.; Park, S. C.; Lee, J.-G.; Kang, H. *J. Chem. Phys.* **2000**, *112*, 8660.
10. Park, S.-C.; Kang, H.; Lee, S. B. *Surface Sci.* **2000**, *450*, 117.
11. (a) Yoon, H. G. *et al*. *J. Vac. Sci. Tech. A* **2000**, *18*, 1464. (b) Liu, W. L. *et al*. *Thin Solid Films* **2004**, *461*, 266.
12. Kang, H.; Shin, T.-H.; Park, S.-C.; Kim, I. K.; Han, S.-J. *J. Am. Chem. Soc.* **2000**, *122*, 9842 .
13. Park, S.-C.; Pradeep, T.; Kang, H. *J. Chem. Phys.* **2000**, *113*, 9373.
14. Park, S.-C.; Maeng, K.-W.; Pradeep, T.; Kang, H. *Angew. Chem. Int. Ed.* **2001**, *40*, 1497.
15. Park, S.-C.; Maeng, K.-W.; Pradeep, T.; Kang, H. *Nucl. Instrum. Methods in Phys. Res. B* **2001**, *182*, 193.
16. Han, S-J.; Lee, C.-W.; Hwang, C.-H.; Lee, K.-H.; Yang, C.; Kang, H. *Bull. Korean Chem. Soc.* **2001**, *22*, 883.
17. (a) Hwang, C.-H.; Lee, C.-W.; Kang, H.; Kim, C. M. *Surface Sci.* **2001**, *490*, 144. (b) Kang, H.; Lee, C. W.; Hwang, C. H.; Kim, C. M. *Appl. Surface Sci.* **2003**, *203*, 842.
18. Kim, C. M.; Hwang, C.-H.; Lee, C.-W.; Kang, H. *Angew. Chem. Int. Ed.* **2001**, *41*, 146.
19. Kasi, S. R.; Kang, H.; Sass, C. S.; Rabalais, J. W. *Surf. Sci. Rep*. **1989**, *10*, 1.
20. Morris, M. R.; Riederer, D. E.; Winger, B. E., Jr.; Cooks, R. G.; Ast, T.; Chidsey, C. E. D. *Int. J. Mass Spectrom. Ion Poc.* **1992**, *122*, 181.
21. Cooks, R. G.; Ast, T.; Pradeep, T.; Wysocki, V. *Acc. Chem. Res.* **1994**, *27*, 316.
22. Murata, Y. *Unimolecular and Bimolecular Reaction Dynamic*; Ng, C. Y., Baer, T., Powis, I., Eds.; John Wiley & Sons: 1994; Chapter 9.
23. Han, S-J.; Lee, C.-W.; Yoon, H.; Kang, H. *J. Chem. Phys.* **2002**, *116*, 2684.
24. Kim, Y. K.; Park, S. C.; Kim, J. H.; Lee, C. W.; Kang, H. *J. Phys. Chem. C* **2008**, *112*, 18104.
25. Kim, Y. K.; Kim, S. K.; Kim, J. H.; Kang, H. *J. Phys. Chem. C* **2009**, *113*, 16863.
26. Kim, S. K.; Kang, H. *J. Phys. Chem. Lett.* **2010**, *1*, 3085-3089.
27. Kang, H. *Acc. Chem. Res.* **2005**, *38*, 893.
28. Jung, K. H.; Park, S. C.; Kim, J. H.; Kang, H. *J. Chem. Phys.* **2004**, *121*, 2758.
29. Park, S. C.; Pradeep, T.; Kang, H. *J. Chem. Phys.* **2000**, *113*, 9373.
30. Kim, J. H.; Shin, T.; Jung, K. H.; Kang, H. *ChemPhysChem* **2005**, *6*, 440.
31. Kim, J. H.; Kim, Y. K.; Kang, H. *J. Phys. Chem. C* **2007**, *111*, 8030.
32. Park, S. C.; Jung, K. H.; Kang, H. *J. Chem. Phys.* **2004**, *121*, 2765.
33. Park, S. C.; Maeng, K. W.; Pradeep, T.; Kang, H. *Angew. Chem. Int. Ed.* **2001**, *40*, 1497.
34. Park, S. C.; Kang, H. *J. Phys. Chem. B* **2005**, *109*, 5124.
35. Park, S. C.; Kim, J. K.; Lee, C. W.; Moon, E. S.; Kang, H. *ChemPhysChem* **2007**, *8*, 2520.
36. Lee, C. W.; Lee, P. R.; Kang, H. *Angew. Chem. Int. Ed.* **2006**, *45*, 5529.
37. Lee, C. W.; Lee, P. R.; Kim, Y. K.; Kang, H. *J. Chem. Phys.* **2007**, *127*, 084701.
38. Moon, E. S.; Lee, C. W.; Kang, H. *Phys. Chem. Chem. Phys.* **2008**, *10*, 4814.
39. Moon, E. S.; Lee, C. W.; Kim, J. K.; Park, S. C.; Kang, H. *J. Chem. Phys*. **2008**, *128*, 191101.
40. Kim, J. H.; Kim, Y. K.; Kang, H. *J. Chem. Phys.* **2009**, *131*, 044705.
41. Moon, E. S.; Yoon, J.; Kang, H. *J. Chem. Phys.* **2010**, *133*, 044709.
42. Park, S. C.; Maeng, K. W.; Kang, H. *Chem.-Eur. J.* **2003**, *9*, 1706.
43. Kim, J. H.; Kim, Y. K.; Kang, H. *J. Phys. Chem. C* **2009**, *113*, 321.
44. Lee, P. R.; Lee, C. W.; Kim, J. K.; Moon, E. S.; Kang, H. *Chem.-Asian J.*, in press.
45. Lee, C. W.; Kim, J. K.; Moon, E. S.; Minh, Y. C.; Kang, H. *Astrophys J.* **2009**, *697*, 428.
46. Moon, E. S.; Kang, H.; Oba, Y.; Watanabe, N.; Kouchi, A. *Astrophys J.* **2010**, *713*, 906.
47. Park, S-C.; Moon, E-S.; Kang, H. *Phys. Chem. Chem. Phys*. **2010**, *12*, 12000.
48. (a) Lahaye, R. J. W. E.; Kang, H. *Phys. Rev. B* **2003**, *67*, 033401. (b) Lahaye, R. J. W. E. *Surf. Sci.* **2010**, *604*, 1135.
49. Han, S.-J.; Lee, C.-W.; Lahaye, R. J. W. E.; Kang, H. *Surf. Sci*. **2003**, *538*, 184.
50. Lahaye, R. J. W. E.; Kang, H. *ChemPhysChem* **2004**, *5*, 697.
51. Hahn, J. R.; Lee, C.-W.; Han, S. J.; Lahaye, R. J. W. E.; Kang, H. *J. Phys. Chem. A* **2002**, *106*, 9827.
52. Lee, C.-W.; Lee, P.-R.; Lahaye, R. J. W. E.; Kang, H. *Phys. Chem. Chem. Phys*. **2009**, *11*, 2268.
53. Kim, J.-H.; Lahaye, R. J. W. E.; Kang, H. *Surf. Sci*. **2007**, *601*, 434.
54. Heiland, W. *Principles of Low Energy Ion Scattering, Vacuum* **1982**, *32*, 539.
55. Rabalais, J. W. *Principles and Applications of Ion Scattering Spectrometry*; Wiley-Interscience: 2003.
56. Lahaye, R. J. W. E.; Kang, H. *Surface Sci.* **2001**, *490*, 144.
57. Yang, M. C.; Lee, H. W.; Kim, C.; Kang, H. *Surface Sci.* **1996**, *357*, 595.
58. Lee, H. W.; Kang, H. *Bull. Korean Chem. Soc.* **1995**, *16*, 101.
59. Bazarbayev, N. N.; Evstifeev, V. V.; Krylov, N. M.; Kubryaschova, L. B. *Soviet. J. Surface* (*Russian*) **1988**, *9*, 170.
60. Evstifeev, V. V.; Ivanov, I. V. *Surface Sci.* **1989**, *217*, L373.
61. Kim, C.; Kang, H.; Park, S. C. *Nucl. Instrum. Methods in Phys. Res. B* **1995**, *95*, 171.
62. Kolodney, E.; Amirav, A.; Elber, R.; Gerber, R. B. *Chem. Phys. Lett.* **1985**, *113*, 303.
63. Kim, C.; Han, J. R.; Kang, H. *Surface Sci.* **1994**, *320*, L76.
64. Shin, T.; Kim, K. N.; Lee, C.W.; Shin, S. K.; Kang, H. *J. Phys. Chem. B* **2003**, *107*, 11674.
65. Salmeron, M.; Somorjai, G. A. *J. Phys. Chem*. **1982**, *86*, 341.
66. Zaera, F.; Janssens, T. V. W.; Ofner, H. *Surf. Sci*. **1996**, *368*, 371.
67. Sheppard, N. *Ann. Rev. Phys. Chem.* **1988**, *39*, 589.
68. Buch, V.; Sadlej, J.; Aytemiz-Uras, N.; Devlin, J. P. *J. Phys. Chem. A* **2002**, *106*, 9374.
69. Molina, M. J.; Tso, T. L.; Molina, L. T.; Wang, F. C. Y. *Science* **1987**, *238*, 1253.